甲第A 310 号証

Unclassified

NEA/CSNI/R(2003)18

Organisation de Coopération et de Développement Economiques
Organisation for Economic Co-operation and Development

22-Dec-2003

English - Or. English

NUCLEAR ENERGY AGENCY
COMMITTEE ON THE SAFETY OF NUCLEAR INSTALLATIONS

OECD/NEA WORKSHOP ON THE RELATIONS BETWEEN SEISMOLOGICAL DATA AND SEISMIC ENGINEERING

Istanbul, 16-18 October 2002

JT00156210

Document complet disponible sur OLIS dans son format d'origine
Complete document available on OLIS in its original format

NEA/CSNI/R(2003)18
Unclassified

English - Or. English

OECD Workshop on the Relations Between Seismological DATA and Seismic Engineering Istanbul, 16-18 October 2002

OECD Workshop on the Relations Between Seismological DATA and Seismic Engineering Istanbul, 16-18 October 2002

C. Table of contents

The name of the speaker is in italic

NEA/CSNI/R(2003)18

OECD Workshop on the Relations Between Seismological DATA and Seismic Engineering Istanbul, 16-18 October 2002

RESPONSE SPECTRA FOR DESIGN PURPOSE OF STIFF STRUCTURES ON ROCK SITES

Shizuo Noda, Kazuhiko Yashiro
Tokyo Electric Power Company, Japan

Katsuya Takahashi, Masayuki Takemura, Susumu Ohno
Kajima Corporation, Japan

Masanobu Tohdo
Toda Corporation, Japan

Takahide Watanabe
Ohsaki Research Institute, Japan

ABSTRACT

For seismic design of nuclear power facilities, we propose an empirical method for evaluating response spectra and time-dependent features of horizontal and vertical earthquake ground motions on free rock surfaces. A response spectrum of horizontal motion on seismic bedrock is given by a control point in the matrix by four magnitudes M and four equivalent hypocentral distances X_{eq}. The response spectra for other M and X_{eq} are determined by interpolation between values in the matrix. The response spectra of the horizontal and vertical motions on the free rock surface are determined by multiplying the horizontal motion on the seismic bedrock by the amplifications of horizontal and vertical motions due to surface layers, which are given as functions of S- and P-wave velocities on the free rock surface, respectively. The proposed evaluation method adequately explains near-source observation records.

Introduction

Earthquake ground motion evaluation methods used for seismic design of structures are roughly classified into empirical, semi-empirical, and theoretical methods [1]. Empirical methods have been widely used as a standard for calculating the response spectrum to be used for seismic design of nuclear power facilities (e.g., Reference 2). This paper discusses and proposes an empirical method for evaluating the response spectra of horizontal and vertical earthquake ground motions on the surfaces of rock mostly composed of Tertiary or older strata, as a reasonable method for establishing a design-basis earthquake ground motion for seismic design of nuclear power facilities.

The earthquake ground motion evaluation method proposed here uses the earthquake magnitude, equivalent hypocentral distance, and elastic wave velocity on the ground at the evaluation point as evaluation parameters. The method is organized so as to reflect, as accurately as possible, actual earthquake ground motion observations. The major features of the method are that (1) it empirically evaluates earthquake ground motion amplification by the surface layers overlaying seismic bedrock using the elastic wave velocity on the ground at an evaluation point, (2) it includes the effect of the extension of the fault on earthquake ground motion so that it can be applied to near-source regions, (3) it can evaluate earthquake ground motion with periods from 0.02 to 5 seconds, which are longer than those in Ref. 2, and (4) it can evaluate both horizontal and vertical motions.

Response Spectra of Earthquake Ground Motion on Free Rock Surface

The response spectra of horizontal and vertical ground motions with periods from 0.02 to 5 seconds on free rock surfaces are evaluated by multiplying the horizontal earthquake ground motion on seismic bedrock by the amplifications of horizontal and vertical motion due to surface layers. Figure 1 shows a schematic flowchart for evaluating the horizontal ground motion.

Horizontal Ground Motion on Seismic Bedrock

The response spectrum S_b (T) of a horizontal earthquake ground motion on seismic bedrock, which is the acceleration response spectrum (cm/s^2) with a damping factor of 5%, is obtained from the pseudo-velocity response spectrum pSv (T) (cm/s) of the period T (s) represented by the control point in Table 1. To determine a control point pSv from an arbitrary magnitude M (the Japan Meteorological Agency Magnitude (JMA) or its equivalent) and an equivalent hypocentral distance X_{eq} that are not directly found in Table 1, $\log pSv$ is interpolated by M first and then by $\log X_{eq}$.

Here, the equivalent hypocentral distance X_{eq} (km) is the distance between an evaluation point and a point source that would produce the same seismic wave energy as the total seismic wave energy that arrives at the evaluation point radiated from the extended fault plane. This is given by [3]

$$X_{eq}^{-2} = \int e_m X_m^{-2} ds \Big/ \int e_m ds, \qquad (1)$$

where X_m is the distance (km) from the evaluation point to each small segment m in the fault plane, e_m is the relative distribution of seismic wave energy released from each segment m, and ds is the segment area (km^2).

e_m is the distribution of seismic wave intensity released from the fault plane in a period range for response spectrum evaluation. Although it has energy dimensions here, a relative distribution can be used instead. Therefore, the distribution of the square of the slip D_m can substitute for the e_m distribution. Because such a distribution is rarely predicted before an earthquake, calculations can

assume that e_m is uniformly distributed (i.e., constant) over the fault plane. Figure 2 illustrates the pseudo-velocity response spectrum for each control point in Table 1.

Horizontal Ground Motion on Free Rock Surface

The response spectrum of the horizontal ground motion on the free rock surface at the control point with a specified period is calculated as follows. We multiply the horizontal ground motion spectrum on the seismic bedrock for the control point by the amplification of horizontal motion due to the surface layers. The amplification is a function of both the S-wave velocity at the free rock surface and the dominant period of the surface layers between the seismic bedrock and the free rock surface.

$$S_h(T_i) = S_b(T_i) \bullet \alpha_h(T_i) \bullet \beta_h(T_i) \tag{2}$$

where $S_h(T_i)$ is the response spectrum (cm/s^2) of horizontal earthquake ground motion on the free rock surface, T_i is the period of control points from A to H in Table 1, $S_b(T_i)$ is the response spectrum (cm/s^2) of horizontal earthquake ground motion on seismic bedrock from Table 1, and $\alpha_h(T_i)$ and $\beta_h(T_i)$ are amplifications of horizontal motion by the surface layers expressed by Eq. (3) below.

The amplifications of seismic waves due to the surface layers overlaying the seismic bedrock depending on the S-wave velocity of the ground and the dominant period are given by the equations below

$$\alpha_h(T_i) = \begin{cases} (V_s/V_{sb})^{-\delta_h(T_i)} & (T_i \le T_{sl}) \\ (V_s/V_{sb})^{-\delta_h(T_{sl})} & (T_i > T_{sl}) \end{cases}, \quad \beta_h(T_i) = \begin{cases} 1 & (T_i \le T_{sl}) \\ (T_i/T_{sl})^{-\log(\sigma_h(T_{sl}))} & (10T_{sl} > T_i > T_{sl}) \\ 10^{-\log(\sigma_h(T_{sl}))} & (T_i \ge 10T_{sl}) \end{cases} \tag{3}$$

where V_s is the S-wave velocity (km/s) of the free rock surface, V_{sb} is the S-wave velocity (km/s) of the seismic bedrock, T_{sl} is the dominant period of horizontal ground motion caused by the surface layers overlaying the seismic bedrock, and $\delta_h(T_i)$ is the coefficient given in Table 2.

Vertical Ground Motion on Free Rock Surface

The response spectrum of the vertical ground motion on the free rock surface at the control point with a specified period is calculated as follows. We multiply the horizontal ground motion spectrum at the seismic bedrock for the control point by the amplification of vertical motion due to the surface layers. The amplification is a function of both the P-wave velocity at the free rock surface and the dominant period of the surface layer between the seismic bedrock and the free rock surface.

$$S_v(T_i) = S_b(T_i) \bullet \alpha_v(T_i) \bullet \beta_v(T_i) \tag{4}$$

where $S_v(T_i)$ is the response spectrum (cm/s^2) of vertical earthquake ground motion on the free rock surface, and $\alpha_v(T_i)$ and $\beta_v(T_i)$ are amplifications of vertical motion by the surface layers expressed by Eq. (5) below.

The amplifications of seismic waves due to the surface layers overlaying the seismic bedrock depending on the P-wave velocity of the ground and the dominant period are given by the equations below.

$$\alpha_v(T_i) = \alpha_{bv}(T_i) \begin{cases} (V_p/V_{pb})^{-\delta_v(T_i)} & (T_i \le T_{pl}) \\ (V_p/V_{pb})^{-\delta_v(T_{pl})} & (T_i > T_{pl}) \end{cases}, \quad \beta_v(T_i) = \begin{cases} 1 & (T_i \le T_{pl}) \\ (T_i/T_{pl})^{-\log\{\sigma_v(T_{pl})/\sigma_{bv}(T_{pl})\}} & (10T_{pl} > T_i > T_{pl}) \\ 10^{-\log\{\sigma_v(T_{pl})/\sigma_{bv}(T_{pl})\}} & (T_i \ge 10T_{pl}) \end{cases} \tag{5}$$

where V_p is the P-wave velocity (km/s) of the free rock surface, V_{pb} is the P-wave velocity (km/s) of the seismic bedrock, T_{pl} is the dominant period of the vertical ground motion caused by the surface layers on the seismic bedrock, $\delta_v(T_i)$ is a coefficient given in Table 2, and $\alpha_v(T_i)$ is the vertical-to-horizontal response spectral ratio on the seismic bedrock given in Table 2.

Table 2 assumes V_{sb} = 2.2 km/s and V_{pb} = 4.2 km/s. When V_s or V_p of the free rock surface exceeds these values, we use instead V_s = 2.2 km/s or V_p = 4.2 km/s, respectively. Figure 3 shows calculation examples of amplification by surface layers of the horizontal and vertical motions. When T_{sl} or T_{pl} does not equal the periods of the control points shown in Table 1, new control points for them are added. From the spectrum obtained above, the response spectrum for a period not equal to the period of the control points is determined by interpolation along a straight line in a diagram where the abscissa is the logarithm of the period and the ordinate is the logarithm of the pseudo-velocity response spectrum.

Time Dependent Features of Earthquake Ground Motion on Free Rock Surface

The amplitude envelope in the time domain $E(t)$ of horizontal and vertical ground motions on the free rock surface is calculated as an envelope with a build-up section from 0 to t_B, a strong-shaking section from t_B to t_C, and a coda section from t_C to t_D as shown in Fig. 4. The envelope function is

$$E(t)=(t/t_B)^2 \ (0<t\le t_B),\ E(t)=1 \ (t_B<t\le t_C),\ E(t)=e^{\ln(0.1)\cdot(t-t_C)/(t_D-t_C)} \ (t_C<t\le t_D) \qquad (6)$$

The duration t_B (s) of the build-up section and the duration $t_C - t_B$ (s) of the strong-shaking section are calculated as functions of the magnitude M. The duration $t_D - t_C$ (s) of the coda section is a function of both the magnitude M and the equivalent hypocentral distance X_{eq}. These durations are expressed by Eq. (7). Figure 4 shows examples of the envelopes.

$$t_B=10^{0.5M-2.93},\ t_C-t_B=10^{0.3M-1.0},\ t_D-t_C=10^{0.17M+0.54\log X_{eq}-0.6} \qquad (7)$$

Response Spectra for Different Damping Factors

When the damping factor is not 5%, the response spectra of the horizontal and vertical ground motions on the free rock surface for the period of the control point are calculated by multiplying the control point's response spectra for the horizontal and vertical ground motions on the free rock surface by a correction coefficient as a function of the damping factor

$$S_h(T_i,h)=S_h(T_i)\cdot\eta(T_i,h),\ S_v(T_i,h)=S_v(T_i)\cdot\eta(T_i,h) \qquad (8)$$

where $S_h(T_i, h)$ and $S_v(T_i, h)$ are the response spectra of the horizontal and vertical ground motions, respectively, on the free rock surface for the damping factor h. $\eta(T_i, h)$ is the correction coefficient of the response spectrum for the damping factor h, which is expressed by Eq. (9). Figure 5 shows examples of the correction coefficient.

$$\eta(T_i,h)=\begin{cases}1/\left\{1+a\cdot(h-0.05)\cdot\exp\left(-b\cdot T_i/T_{eq}\right)\right\}^{1/2} & (T_i=T_C,\cdots,T_H)\\ 1/\left\{1+a\cdot(h-0.05)\cdot\exp\left(-b\cdot T_C/T_{eq}\right)\right\}^{1/2} & (T_i=T_B)\\ 1 & (T_i=T_A)\end{cases} \qquad (9)$$

where T_{eq}, which is given by Eq. (10) below, is the duration for which an acceleration wave is assumed to have a constant intensity of the strong-shaking section and its total power equals that of the envelope's acceleration wave. Constants a and b are given by Eq. (11) below.

$$T_{eq} = 10^{0.3M-1.0} + 0.2 \cdot 10^{0.17M+0.54\log X_{eq}-2.6} \quad (10)$$

$$a=15,\ b=2.0\ (h<0.05),\ a=13,\ b=5.0\ (h>0.05) \quad (11)$$

On Application of the Proposed Method

Database

The evaluation method proposed in the above sections is based on an average response spectrum from references 4 and 5 obtained from regression analyses of 107 records (321 components) of 44 earthquakes observed in Tertiary or older strata. The standard error in the regression analysis was nearly independent of period and about 0.23 in common log scale (base 10).

At the above observation points, the S-wave velocity V_s ranged from 0.5 to 2.7 km/s and the P-wave velocity V_p ranged from 1.7 to 5.5 km/s. These values closely correspond to those of the free rock surface (V_s of approximately 0.7 km/s or larger [2]) and the seismic bedrock (with V_s of about 3.0 km/s [6]). This evaluation method is applicable to rock sites with elastic wave velocities within the above range. Its application to rock sites with other elastic wave velocities requires special attention, such as reinvestigation of the amplification by the surface layers. In addition, when many observation records are collected at an evaluation point, the amplification by the surface layers peculiar to the site can be evaluated by comparing the observation records with the estimates on the seismic bedrock by the present evaluation method. However, as a rule, recorded data to be used in this case should be within the range of data used by this evaluation method.

The range of data used in the regression analysis is shown in Table 3. The range of magnitudes for the control points was up to $M = 8.5$, as shown in Table 1, and the control points corresponding to $M > 7.0$ were determined by extrapolation. Nevertheless, it was shown that results obtained from the regression equation agreed closely with records of large earthquakes inside and outside Japan [4,5]. Therefore, the control points at $M = 8.0$ were determined from this regression equation [7]. However, because there were no observation records for comparison, the control points for $M = 8.5$ were extrapolated from those for $M = 8.0$ by a theoretical examination based on a fault model. The time-dependent characteristics and the response spectrum correction coefficient due to damping factor are also based on analysis of earthquake records in the above database.

As all hypocentral depths of the earthquake in the regression data were less than 60 km, and about 80 % of the earthquakes occurred at subduction zones, the estimates by the proposed method are strongly affected by the strong-motion characteristics of subduction-zone earthquakes. Accordingly, for shallow earthquakes at inland active faults or deep earthquakes within a subducting slab, or for near-source regions at which the long-period pulse become predominant, the following corrections or considerations become necessary.

Evaluation of shallow inland earthquakes

Using the regression data and K-NET data (the K-NET has been widely installed in Japan since the Kobe earthquake of 1995 [8]), we divided these data into two categories: data of subduction-zone earthquakes and data of shallow inland earthquakes. We took the spectral ratios between the observations and the estimates by the present method for all categorized data.

The data ranges used for analysis are summarized in Table 3. M-Xeq distributions and the epicentral map of the data are shown in Fig. 6 and Fig. 7. The stations at which shear-wave velocity within 20m-depth exceeds 0.7 km/s were used. To avoid the effect of soil response by the soft layers shallower than the layer of Vs≥0.7 km/s, the period range longer than twice the soft layer's predominant period were analyzed.

Figure 8 shows the average and the average plus/minus the standard deviation of the spectral ratios. The estimates agree with the observations for the subduction-zone data as the average is close to one, while the estimates for the shallow inland earthquake overestimate the observations. Accordingly, the present method explains the subduction-zone data well, as expected, and corrections become necessary in application to shallow inland earthquakes. As the spectral ratios shown in Fig. 8 are nearly independent of M and X_{eq}, we propose the correction coefficient ζ for the shallow inland earthquakes based on this spectral ratio as

$$\zeta(T_i)=0.6\ (T_i \le T_g),\ \zeta(T_i)=10^{\log(0.6)\cdot\log(T_H/T_i)/\log(T_H/T_g)}\ (T_g < T_i). \tag{12}$$

This result means that the amplitudes of the shallow inland earthquake data are smaller than those of the subduction-zone earthquake data. This is probably because (1) the JMA magnitude scale, which is used in this study, tends to be overestimated for shallow inland earthquakes compared with its proper earthquake scale [9], and (2) the radiation strength of the short-period amplitude of shallow earthquakes is smaller than that of deep earthquakes because of the different rigidities of the source media.

Evaluation of Intermediate Depth Earthquakes

Reference 10 reports that the short-period amplitude for an earthquake with a focal depth deeper than 60 km is greater than that for shallower earthquakes, even for the same magnitude and source-to-site distance. It also reports that short-period amplitudes for such intermediate-depth earthquakes have regional variations. Therefore, the evaluation of the response spectrum for an intermediate-depth earthquake needs a site-dependent investigation based on the records observed around the evaluation site.

Evaluation of Near-Fault Rupture Directivity (NFRD) Effect

The dominance of the fault-normal component with periods from one to a few seconds has been reported in the near-source records of shallow inland earthquakes such as the 1995 Hyogo-ken Nanbu (Kobe) earthquake, Japan. The reason for this phenomenon is that the horizontal component perpendicular to the fault strike grows larger in the direction of rupture propagation due to the combined effects of rupture propagation and the fault mechanism. Therefore, attention must be paid to such effects in the evaluation of near-fault ground motion. Reference 11 describes the range in which the NFRD effect is dominant and also describes a method for correcting the response spectrum for this effect. For correction of the NFRD effect based on Reference 11, the corrected spectrum can be obtained by multiplying the correction factor λ, where

$$\lambda(T_i)=1\ (T_i \le T_D),\ \lambda(T_i)=10^{\log(2.5)\cdot\log(T_i/T_D)/\log(T_H/T_D)}\ (T_D < T_i). \tag{13}$$

by the response spectrum obtained by the evaluation method proposed in this paper.

Figure 9 compares the response spectra of the observation record at Kobe University during the Hyogo-ken Nanbu earthquake of 1995 and the record at Sakarya during the Kocaeli earthquake of 1999 with the estimates by this evaluation method. At Sakarya, the NS (Fault-normal) component was not observed. As both were shallow inland earthquakes, the correction by Eq.(12) was applied in the

estimation. In spite of the fact that the stations are located very close to the faults, the proposed method can explain the observation records well. Still, by the correction of Eq. (13), the correspondence between the estimate and the observation improve for the NS (Fault-normal) component of Kobe Univ.

Conclusions

We proposed a method for empirically evaluating response spectra and time-dependent features of horizontal and vertical earthquake ground motions on a free rock surface, based on analysis of observation records on rock. This method should be useful for calculating design-basis earthquake ground motion used for seismic design of nuclear power facilities. We also showed that the evaluation method could adequately explain observations of near-source regions.

Acknowledgments

This study was jointly funded by ten electric power companies in Japan. Because of their helpful guidance, we also thank the late Emeritus Prof. Syunitiro Omote of Kyushu Industrial University, former Prof. Makoto Watabe of Keio University, Prof. Motohiko Hakuno of Kogyokusha College of Technology, and Emeritus Prof. Hiroyoshi Kobayashi of Tokyo Institute of Technology.

References

1. The Architectural Institute of Japan, "Earthquake Motion and Ground Conditions," Part III. Prediction of Strong Ground Motion and Its Application to Earthquake Engineering, Chapter 1, Simulation and Prediction of Strong Ground Motion, The Architectural Institute of Japan, 1993.
2. Hisada, T., Ohsaki, Y., Watabe, M. and Ohta, T., "Design Spectra for Stiff Structures on Rock," Proc. of the 2nd International Conference on Microzonation for, Vol. III, pp.1187-1198, 1978.
3. Ohno, S., Ohta, T., Ikeura, T. and Takemura, M., "Revision of Attenuation Formula Considering the Effect of Fault Size to Evaluate Strong Motion Spectra in Near Field," Tectonophysics, Vol. 218, pp.69-81, 1993.
4. Takahashi, K., Takemura, M., Tohdo, M, Watanabe, T. and Noda, S., "Empirical Response Spectral Attenuations on the Rocks with Vs = 0.5 to 3.0 km/s in Japan," Proc. of the 10th Japan Earthquake Engineering Symposium, pp.547-552, 1998 (in Japanese with English Abstract).
5. Kawano, H., Takahashi, K., Takemura, M., Tohdo, M., Watanabe, T. and Noda, S., "Empirical Response Spectral Attenuations on the Rocks with Vs=0.5 to 3.0 km/s in Japan," Proc. of the 12th World Conference on Earthquake Engineering, Reference No. 953, 2000.
6. Kobayashi, H. and Midorikawa, S., "A Semi-Empirical Method for Estimating Response Spectra of Near-Field Ground Motions with regard to Fault Rupture," Proc. of the 7th European Conference on Earthquake Engineering, pp.161-168, 1982.
7. Nishimura, I., Noda, S., Takahashi, K., Takemura, M., Ohno, S., Tohdo, M. and Watanabe, T., , "Response Spectra for Design Purpose of Stiff Structures on Rock Sites," Transactions, SMiRT 16, Paper # 1133, 2001.
8. Kinoshita, S., "Kyoshin Net (K-NET),"Seism. Res. Lett., 69, pp.309-332, 1998.
9. Takemura, M., "Magnitude.- Seismic Moment Relations for the Shallow Earthquakes in and around Japan, " Zisin, 2nd Series, 43, pp.257-265, 1990 (in Japanese with English Abstract).
10. Kato, K., Takemura, M., Ikeura, T. and Yashiro, K., "Excitation Strength of High-frequency Seismic Motion due to Intermediate Depth Earthquakes," Proc. of the 10th Japan Earthquake Engineering Symposium, pp.673-678, 1998 (in Japanese with English Abstract).
11. Ohno, S., Takemura, M. and Kobayashi, Y., "Effects of Rupture Directivity on Near-Source Strong Motions," Proc. of the 2nd International Symposium on the Effects of Surface Geology on Seismic Motion, pp. 1163-1170, 1998.

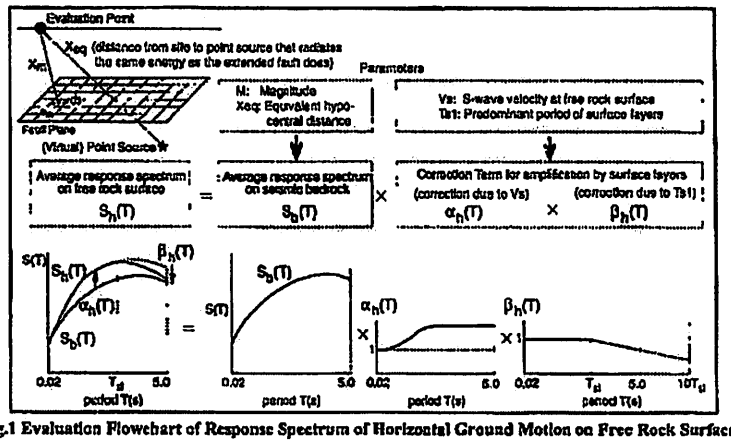

Fig.1 Evaluation Flowchart of Response Spectrum of Horizontal Ground Motion on Free Rock Surface

Table 1. Control Points of Horizontal Earthquake Motion on Seismic Bedrock

Field	M	Xeq (km)	Coordinates of Control Points pSv (cm/s)							
			A	B	C	D	E	F	G	H
			TA(s)	TB(s)	TC(s)	TD(s)	TE(s)	TF(s)	TG(s)	TH(s)
			0.02	0.09	0.13	0.3	0.6	1	2	5
Very Near	8.5	40	1.62	18.44	27.32	47.87	68.05	64.66	53.52	40.08
	8	25	1.69	20.05	28.96	48.22	67.80	65.25	52.51	38.35
	7	12	1.40	17.20	24.84	33.88	43.42	36.42	25.15	17.85
	6	6	1.04	12.82	18.51	21.84	23.17	17.41	9.64	3.88
Near	8.5	80	0.73	7.36	11.43	22.92	34.79	32.58	27.60	21.96
	8	50	0.67	7.45	11.17	20.05	28.65	27.06	22.70	17.19
	7	20	0.78	9.44	13.64	19.10	24.83	20.69	14.48	10.37
	6	8	0.77	9.45	13.65	16.23	17.18	12.73	7.16	2.89
Inter mediate	8.5	160	0.28	2.22	3.67	9.45	15.17	14.83	13.64	12.26
	8	100	0.32	3.08	4.86	10.27	16.04	14.96	12.73	10.37
	7	50	0.23	2.65	4.01	6.02	7.64	6.68	4.87	3.64
	6	25	0.21	2.49	3.60	4.54	4.84	3.98	2.07	0.86
Far	8.5	200	0.18	1.44	2.49	6.87	11.17	11.17	10.67	10.04
	8	200	0.10	0.80	1.35	3.82	6.21	6.21	5.93	5.58
	7	125	0.046	0.43	0.70	1.34	1.81	1.59	1.26	1.05
	6	78	0.041	0.45	0.65	0.65	1.03	0.80	0.49	0.22

The value of pSv is pseudo-velocity response spectrum with a damping factor of 5%.

Table 2. Coefficients $\delta_h(T)$, $\delta_v(T)$, and $\alpha_{bv}(T)$

	A	B	C	D	E	F	G	H
	TA(s)	TB(s)	TC(s)	TD(s)	TE(s)	TF(s)	TG(s)	TH(s)
	0.02	0.09	0.13	0.3	0.6	1	2	5
$\delta_h(T)$	0	0.03	0.05	0.35	0.48	0.61	0.80	0.83
$\delta_v(T)$	0.12	0.26	0.42	0.67	0.90	1.03	1.10	1.09
$\alpha_{bv}(T)$	0.58	0.55	0.52	0.59	0.56	0.60	0.70	0.75

The coefficients are common for all combinations of M and Xeq

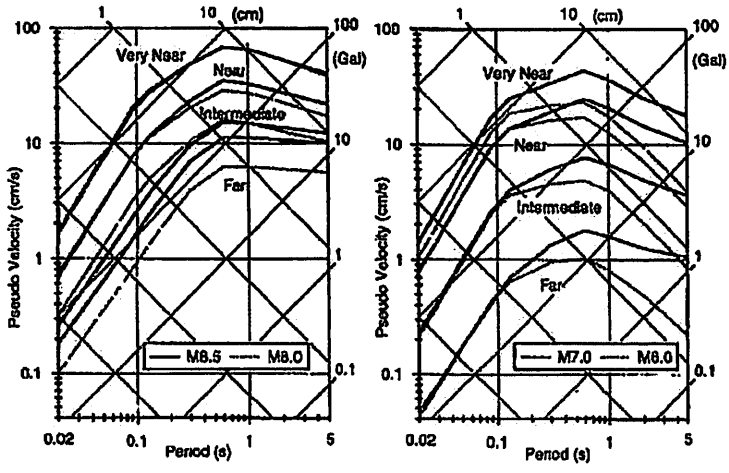

Fig. 2 Response Spectra of Horizontal Earthquake Motions on Seismic Bedrock at the Control Points in Table 1.

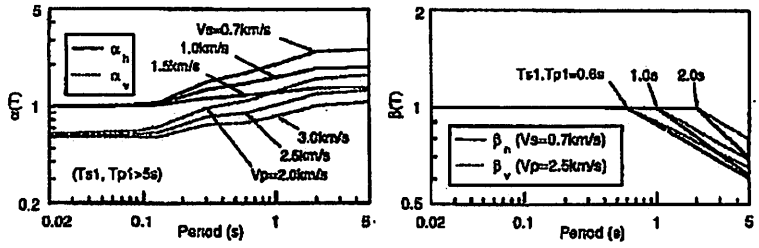

Fig. 3 Calculation Examples of α (T) and β (T) for Horizontal and Vertical Ground Motions

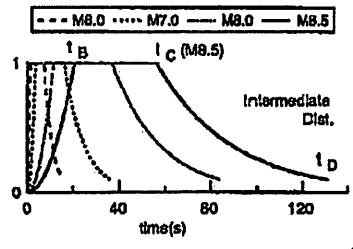

Fig. 4 Time Envelopes at the intermediate distances of the Control Points in Table 1.

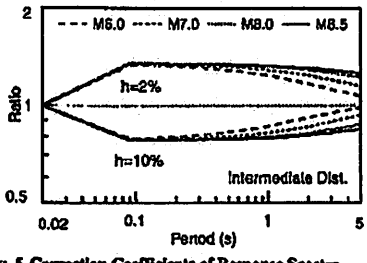

Fig. 5 Correction Coefficients of Response Spectra for Different Damping Factors at the Intermediate distances of the Control Points in Table 1.

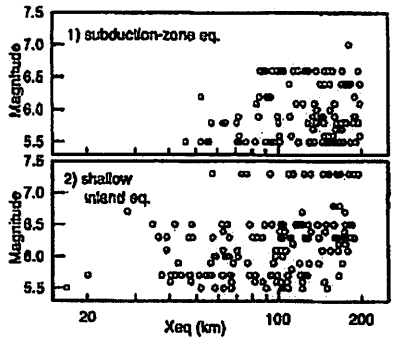

Fig. 6 M-Xeq distribution of the data used for analysis in Fig. 8.

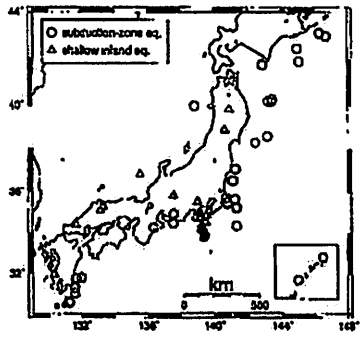

Fig. 7 Epicenter distribution of the earthquakes used for analysis in Fig. 8.

Table 3. Data Range used for analysis

	Data for regression analysis in Ref. 4,5	Data for applicability check in Ref.7	Data used in this paper	
			subduction-zone eq.	shallow inland eq.
Magnitude	5.5 - 7.0	5.4 - 8.1	5.5 - 7.0	5.5 - 7.3
Xeq (km)	28 - 202	14 - 218	46 - 199	17 - 195
Vs (m/s)	≥500	≥550	≥700	≥500
Number of Records	107	37	124	170

All data satisfy 1) Focal depth ≤ 60km, 2) Observation sites belong to stratum of tertiary or older.

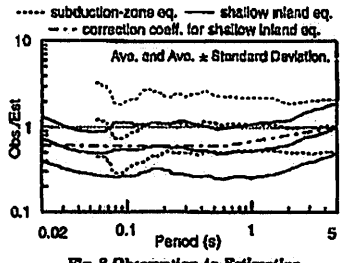

Fig. 8 Observation-to-Estimation Response Spectral Ratios

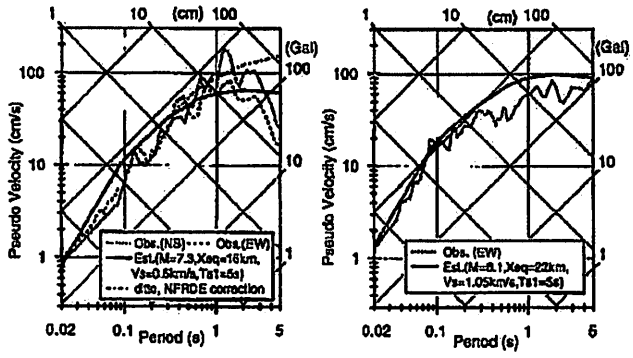

(1) 1995 Hyogo-ken Nanbu (Kobe) Eq., Kobe Univ. station, Japan

(2) 1999 Kocaeli Eq., Sakarya station, Turkey

Fig. 9 Application Examples of the Evaluation Method to Near-Source Records.

岩盤上の剛構造物に対する設計用応答スペクトル

野田静男，八代和彦
東京電力

高橋克也，武村雅之，大野晋
鹿島建設

藤堂正喜
戸田建設

渡辺孝英
大崎総合研究所

要約

原子炉施設の耐震設計に用いる基準地震動の合理的な策定方法として，岩盤での地震動観測記録を分析した結果に基づいて，解放基盤表面における水平・上下地震動の応答スペクトルとその経時特性の経験的な評価法を提案した。地震基盤の水平地震動の応答スペクトルはマグニチュード M が４種類，等価震源距離 Xeq が４種類のマトリックス上のコントロールポイントで与えられ，任意の M と Xeq についてはコントロールポイント間の内挿により求める。解放基盤表面の水平・上下地震動の応答スペクトルは，地震基盤における水平地震動を共通として，これに解放基盤表面のＳ波およびＰ波速度の関数として与えた水平動および上下動の地盤増幅率を乗じて求める。また，本評価法は震源近傍の観測記録を良く説明することを示した。

はじめに

構造物の耐震設計に用いる地震動の評価法は，経験的手法，半経験的手法，理論的手法に大きく分けられる[1]。このうち経験的手法による評価は，原子力発電所の耐震設計用応答スペクトルの標準的な算定方法として広く用いられてきた（例えば文献 2)。本論文は，概ね第三紀以前の地層の表面（解放基盤表面[2]）における水平・上下地震動の応答スペクトルとその経時特性の経験的な評価法をまとめたもので，文献 2 と同様に原子炉施設の耐震設計に用いる基準地震動の合理的な策定方法として提案するものである。

本提案の評価法は，マグニチュード，等価震源距離，評価地点の地盤の弾性波速度をパラメータとして地震動を評価するもので，実際に観測された地震動の記録をできるだけ正確に反映するように作成された。その主な特徴は，1）評価地点の地盤の弾性波速度を用いて地震基盤から表層の増幅率を経験的に評価していること，2）震源近傍へ適用するために断層の広がりの効果を考慮していること，3）周期 0.02～5 秒と文献 2 の周期帯よりも長周期領域まで評価できること，4）水平動に加えて上下動も評価可能なことである。

解放基盤表面における地震動の応答スペクトル

解放基盤表面における水平および上下地震動の周期 0.02 秒～5 秒の応答スペクトルは，地震基盤における水平地震動を共通として，これに水平動の地盤増幅率および上下動の地盤増幅率を乗じて求められる。水平地震動の評価の模式図を図 1 に示す。

地震基盤における水平地震動

地震基盤における水平地震動の応答スペクトル $S_b(T)$（減衰定数 5%の加速度応答スペクトル(cm/s²)）は，表 1 のコントロールポイントで表わされる周期 T(s)の擬似速度応答スペクトル $pSv(T)$（cm/s）に基づいて得られる。任意のマグニチュード M（気象庁マグニチュードまたはそれに準ずるもの）と等価震源距離 Xeq(km)に対してコントロールポイントの値を求めるには，まず $\log pSv$ を M によって内挿し，ついでこれを $\log Xeq$ によって内挿して，該当する pSv の値を求める。

ここで等価震源距離 Xeq(km)は，広がりをもつ断層面から評価地点に到達する地震波エネルギーの総量と同じ地震波エネルギーを与える点震源までの距離であり，(1)式で与えられる[3]。

$$X_{eq}^{-2} = \int e_m X_m^{-2} ds \Big/ \int e_m ds \qquad (1)$$

ここで，X_m：観測点から断層面の各微小領域 m への距離(km)，e_m：断層面上の各微小領域 m からの地震波エネルギーの相対的放出分布，ds：断層面の微小領域 m の面積(km²)である。

e_m は応答スペクトルの対象周期帯における断層面での地震波エネルギーの相対的放出強度分布であり，エネルギーの次元で表現されているが，相対値を与えるものでも良い。このため，すべり量 D_m の 2 乗値の分布等でも代用することができる。またこれらの分布が地震発生前に予測されている場合は稀であるため，その場合 e_m を断層面上で一様に仮定（e_m

一定）して計算してもよい。図２に表１の各コントロールポイントの擬似速度応答スペクトルを示す。

解放基盤表面における水平地震動

解放基盤表面における水平地震動の応答スペクトルのコントロールポイントは，各コントロールポイントの周期において，地震基盤の水平地震動のコントロールポイントのスペクトル値に解放基盤表面での地盤の S 波速度と地震基盤から解放基盤表面までの地盤の卓越周期の関数で表される水平動の地盤増幅率を乗じて算定する。

$$S_h(T_i) = S_b(T_i) \bullet \alpha_h(T_i) \bullet \beta_h(T_i) \tag{2}$$

ここで，$S_h(T_i)$：解放基盤表面における水平地震動の応答スペクトル(cm/s²)，T_i：表１で与えられるコントロールポイント A～H の周期(s)，$S_b(T_i)$：表１から得られる地震基盤における水平地震動の応答スペクトル(cm/s²)，$\alpha_h(T_i)$，$\beta_h(T_i)$：(3)式で表される水平地震動の地盤増幅率である。

地盤の S 波速度および地盤の卓越周期による地震基盤からの地盤増幅率は以下の式で表される。

$$\alpha_h(T_i) = \begin{cases} (V_s/V_{sb})^{-\delta_h(T_i)} & (T_i \le T_{s1}) \\ (V_s/V_{sb})^{-\delta_h(T_{s1})} & (T_i > T_{s1}) \end{cases}, \quad \beta_h(T_i) = \begin{cases} 1 & (T_i \le T_{s1}) \\ (T_i/T_{s1})^{-\log\{\alpha_h(T_{s1})\}} & (10T_{s1} > T_i > T_{s1}) \\ 10^{-\log\{\alpha_h(T_{s1})\}} & (T_i \ge 10T_{s1}) \end{cases} \tag{3}$$

ここで，V_s:解放基盤表面での地盤のＳ波速度(km/s)，V_{sb}：地震基盤におけるＳ波速度(km/s)，T_{s1}：水平地震動に対する地盤の卓越周期(s)，$\delta_h(T_i)$：表２で与えられる係数である。

解放基盤表面における上下地震動

解放基盤表面における上下地震動の応答スペクトルのコントロールポイントは，各コントロールポイントの周期において，表１から得られる地震基盤の水平地震動のコントロールポイントのスペクトル値に解放基盤表面での地盤の P 波速度と地震基盤から解放基盤表面までの地盤の卓越周期の関数で表される上下動の地盤増幅率を乗じて算定する。

$$S_v(T_i) = S_b(T_i) \bullet \alpha_v(T_i) \bullet \beta_v(T_i) \tag{4}$$

ここで，$S_v(T_i)$：解放基盤表面における上下地震動の応答スペクトル(cm/s²)，$\alpha_v(T_i)$，$\beta_v(T_i)$：(5)式で表される上下地震動の地盤増幅率である。

地盤の P 波速度および地盤の卓越周期による地震基盤からの地盤増幅率は以下の式で表される。

$$\alpha_v(T_i) = \alpha_{bv}(T_i) \begin{cases} (V_p/V_{pb})^{-\delta_v(T_i)} & (T_i \le T_{p1}) \\ (V_p/V_{pb})^{-\delta_v(T_{p1})} & (T_i > T_{p1}) \end{cases}, \quad \beta_v(T_i) = \begin{cases} 1 & (T_i \le T_{p1}) \\ (T_i/T_{p1})^{-\log\{\alpha_v(T_{p1})/\alpha_{bv}(T_{p1})\}} & (10T_{p1} > T_i > T_{p1}) \\ 10^{-\log\{\alpha_v(T_{p1})/\alpha_{bv}(T_{p1})\}} & (T_i \ge 10T_{p1}) \end{cases} \tag{5}$$

ここで，V_p:解放基盤表面での地盤のＰ波速度(km/s)，V_{pb}：地震基盤におけるＰ波速度(km/s)，T_{p1}：上下地震動に対する地盤の卓越周期(s)，$\delta_v(T_i)$：表２で与えられる係数，$\alpha_{bv}(T_i)$：表２で与えられる地震基盤における水平地震動に対する上下地震動の応答スペクトル比であ

る。

表2は V_{sb}=2.2km/s, V_{pb}=4.2 km/s として使うことを想定している。したがって，それらを超える V_s, V_p に対しては，V_s=2.2km/s あるいは V_p =4.2km/s に対する値をそのまま用いるものとする。図3は水平動及び上下動の地盤増幅率の算定例である。

T_{s1} あるいは T_{p1} がコントロールポイントの周期と一致しない場合，この T_{s1} あるいは T_{p1} が新たなコントロールポイントとして追加される。以上によって求められたコントロールポイントのスペクトル値に対して，各コントロールポイント間は，横軸を周期の対数軸，縦軸を速度応答スペクトルの対数軸とした図で直線となるように補間する。

解放基盤表面における地震動の経時特性

解放基盤表面における水平地震動と上下地震動の振幅包絡線 $E(t)$を，図4に示すように立ち上がり部（時間0から t_Bの間），強震部（時間 t_Bから t_Cの間），減衰部（時間 t_Cから t_D の間）から構成される振幅包絡線として算定した。また，振幅包絡線の形状を(6)式のように定めた。

$$E(t)=(t/t_B)^2 \quad (0<t\le t_B),\quad E(t)=1 \quad (t_B<t\le t_C),\quad E(t)=e^{\ln(0.1)\cdot(t-t_C)/(t_D-t_C)} \quad (t_C<t\le t_D) \tag{6}$$

立ち上がり部の継続時間 t_B(s)と強震部の継続時間 t_C - t_B(s)はマグニチュード Mの関数，減衰部の継続時間 t_D - t_C (s)はマグニチュード Mと等価震源距離 Xeqの関数として(7)式で算定した。図4に包絡線の例を示す。

$$t_B=10^{0.5M-2.93},\quad t_C-t_B=10^{0.3M-1.0},\quad t_D-t_C=10^{0.17M+0.54\log X_{eq}-0.6} \tag{7}$$

異なる減衰定数の応答スペクトル

5%以外の減衰定数に対する解放基盤表面における水平及び上下地震動の応答スペクトルは，各コントロールポイントの周期において，解放基盤表面における水平及び上下地震動のコントロールポイントの応答スペクトル値に(8)式で表される減衰定数 h による補正係数を乗じて算定する。

$$S_h(T_i,h)=S_h(T_i)\bullet\eta(T_i,h),\qquad S_v(T_i,h)=S_v(T_i)\bullet\eta(T_i,h) \tag{8}$$

ここで，$S_h(T_i,h)$，$S_v(T_i,h)$はそれぞれ，解放基盤表面における水平地震動・上下地震動の減衰定数 h の応答スペクトル，$\eta(T_i,h)$は(11)式で表される減衰定数 h による応答スペクトルの補正係数である。T_i，$S_h(T_i)$，$S_v(T_i)$は(2)，(4)式の説明を参照されたい。減衰定数 5%の応答スペクトルに対する他の減衰定数 h の応答スペクトルの補正係数は，表1のコントロールポイントの各周期について(9)式で表される。図5に補正係数の例を示す。

$$\eta(T_i,h)=\begin{cases}1\Big/\left\{1+a\bullet(h-0.05)\bullet\exp(-b\bullet T_i/T_{eq})\right\}^{1/2} & (T_i=T_c,\cdots,T_H)\\ 1\Big/\left\{1+a\bullet(h-0.05)\bullet\exp(-b\bullet T_c/T_{eq})\right\}^{1/2} & (T_i=T_B)\\ 1 & (T_i=T_A)\end{cases} \tag{9}$$

ここで T_{eq}は(10)式で与えられ，強震部と同じ強さの加速度波が定常に続くと仮定した際に，その全パワーが包絡線による加速度波と等価になる継続時間である。定数 a，bは(11)式で与えられる。

$$T_{eq} = 10^{0.3M-1.0} + 0.2 \bullet 10^{0.17M+0.54\log X_{eq}-0.6} \tag{10}$$

$$a = 15, b = 2.0 (h < 0.05); a = 13, b = 5.0 (h > 0.05) \tag{11}$$

本評価法の適用について

データベース

本論文の評価式は，第三紀以前の地層で観測された 44 地震 107 記録（321 成分）の回帰分析により得られた平均応答スペクトル（文献 4)5)）に基づいて作成された。回帰分析時の標準誤差は概ね周期によらず常用対数で 0.23 程度であった。

観測点の地盤の弾性波速度の範囲は S 波速度 V_s=0.5～2.7km/s，P 波速度 V_p=1.7～5.5km/s であり，解放基盤から地震基盤（V_s=3.0 程度 [6]）に近い条件の地点まで含むものである。本評価法は基本的にこれらの弾性波速度の範囲内の岩盤で適用可能であり，これらの範囲外の地盤に適用する際には，地盤の増幅率を別途算定するなど特別の注意が必要となる。また，評価地点で多数の観測記録がある場合には，本評価法による地震基盤での地震動評価結果と比較の上，サイト固有の地盤増幅率を評価することができる。その際，用いるデータの範囲は，原則として本評価法で用いたデータの範囲に入ることが望ましい。

回帰分析に用いたデータベースの範囲を表 3 に示す。コントロールポイントのマグニチュードの範囲は表 1 に示すように M8.5 までとなっており，M7 以上は外挿となっている。ただし，回帰式と国内外の大地震記録との対応は良好であることが確認されており [4,6]，M8.0 のコントロールポイントはこの回帰式に基づいて定めている [7]。一方 M8.5 のコントロールポイントについては，比較できる観測記録がないため，M8.0 のコントロールポイントを断層モデルに基づく理論的検討によって外挿して求めている。経時特性及び応答スペクトルの減衰定数による補正係数も，上記のデータベースの地震記録の分析に基づいて定めたものである。

なお，データベースは深さ 60km 以浅の地震のみからなり，そのうち海溝沿いの地震が 8 割程度を占めるため，本評価法は基本的には海溝沿いの地震を対象としたものとなっている。そのため，内陸浅部の活断層で起こる地震や沈み込むプレート内で起こる深い地震，さらに震源近傍で長周期パルスが卓越する場合の評価については，次に示すような補正や考慮が必要となる。

内陸地震の評価

評価式算定に用いた観測データおよび兵庫県南部地震以降に日本全国で設置された K-NET の記録 [8]を対象として，海溝沿いの地震と内陸の浅い地震の記録に分け，それぞれに対して本評価法で求められたスペクトルに対する比を求めた。

用いたデータ範囲を表 3 に，M - X_{eq}分布を図 6 に，震央分布を図 7 に示す。K-NET は深さ 20m 以内に V_s≥700m/s 層が確認されている地点を用いたが，表層軟弱層の影響を除く

ため，軟弱層の卓越周期の2倍以上の周期帯域のみを検討対象とした。

図8は比の平均と標準偏差の範囲を示したものである。海溝沿いの地震では平均は1に近く，記録と良好に対応していること，一方内陸の地震では系統的に過大評価になっていることがわかる。したがって，本評価法はやはり海溝沿いの地震をよく説明するものであり，内陸地震に対しては補正が必要と考えられる。図8に示したスペクトル比は概ねMやX_{eq}によらず共通に得られたことから，このスペクトル比の平均値に基づき，本評価法を内陸の浅い地震に適用する際の補正係数を次式のように設定した。

$$\varsigma(T_i)=0.6 \quad (T_i \le T_E), \qquad \varsigma(T_i)=10^{\log(0.6)\cdot\log(T_H/T_i)/\log(T_H/T_E)} \quad (T_E < T_i) \tag{12}$$

なお内陸地震の振幅が小さい理由としては，1)ここで用いた気象庁マグニチュードMが内陸の浅い地震では地震規模に比べて過大評価されやすいこと[9]，2)浅い地震では深い地震に比べて震源媒質の剛性が低いので，短周期地震波の励起も相対的に小さくなることなどが考えられる。

やや深発地震の評価

文献10によれば，同じマグニチュードと距離に対しても，震源が60kmよりも深い地震の方が浅い地震よりも短周期領域の地震動が大きいと報告されている。したがって，震源が60kmよりも深い地震の評価については，評価地点ごとに観測記録をもとにした評価を別途行う必要がある。

震源近傍での破壊伝播効果の評価

1995年兵庫県南部地震を代表とする内陸地震の震源近傍の観測記録には，断層走向直交方向で周期1～数秒の長周期成分が卓越することが報告されている。これは，断層破壊の伝播と震源メカニズム解の影響により，破壊の進行方向で断層走向と直交する水平動成分が大きくなるためと指摘されており，震源近傍での地震動評価に際してはこのような効果に注意する必要がある。文献11ではこの効果が卓越する範囲と応答スペクトルの補正方法についてまとめられている。その結果に基づいて本評価法の応答スペクトルを補正する場合には，(13)式で与えられる補正係数を乗じて算定できる。

$$\lambda(T_i)=1 \quad (T_i \le T_D), \qquad \lambda(T_i)=10^{\log(2.5)\cdot\log(T_i/T_D)/\log(T_H/T_D)} \quad (T_D < T_i) \tag{13}$$

図9は1995年兵庫県南部地震神戸大と1999年Kocaeli地震Sakaryaについて，観測記録の応答スペクトルと本評価法による推定値を比較したものである。なおSakaryaでは断層直交方向にあたるNS成分が欠測であった。どちらも内陸の浅い地震のため推定の際は(12)式の補正を行っている。これらの記録は断層のごく近傍で得られているが，本評価法による推定値は観測記録をよく説明することがわかる。また(13)式による補正を行うことにより，神戸大の断層直交成分については記録と推定値の対応が良くなることも確認できる。

まとめ

原子炉施設の耐震設計に用いる基準地震動の合理的な策定方法として，岩盤での地震動

観測記録を分析した結果に基づいて，解放基盤表面における水平・上下地震動の応答スペクトルとその経時特性の経験的な評価法を提案した。また，本評価法が震源近傍の観測記録を良く説明することを示した。

謝辞

本研究は10電力共研によるものです。本研究について，故九州産業大学名誉教授表俊一郎先生，前慶応大学教授渡部丹先生，攻玉社工科短期大学教授伯野元彦先生，東京工業大学名誉教授小林啓美先生のご指導をいただきました。記して感謝いたします。

参考文献

1. The Architectural Institute of Japan, "Earthquake and Ground Motions," Part III. Prediction of Strong Ground Motion and Its Application to Earthquake Engineering, Chapter 1, Simulation and Prediction of Strong Ground Motion, The Architectural Institute of Japan, 1993.
2. Hisada, T., Ohsaki, Y., Watabe, M. and Ohta, T., "Design Spectra for Stiff Structures on Rock," Proc. of the 2nd International Conference on Microzonation for Safer Construction, Vol. III, pp.1187-1198, 1978.
3. Ohno, S., Ohta, T., Ikeura, T. and Takemura, M., "Revision of attenuation formula considering the effect of fault size to evaluate strong motion spectra in near field," Tectonophysics. Vol. 218, pp.69-81, 1993.
4. Takahashi, K., Takemura, M., Tohdo, M, Watanabe, T. and Noda, S., "Empirical Response Spectral attenuations on the Rocks with Vs = 0.5 to 3.0 km/s in Japan," in Proc. of the 10th Japan Earthquake Engineering Symposium, pp.547-552, 1998 (in Japanese with English Abstract).
5. Kawano, H., Takahashi, K., Takemura, M., Tohdo, M., Watanabe, T. and Noda, S., "Empirical Response Spectral Attenuations on the Rocks with Vs=0.5 to 3.0 km/s in Japan," Proc. of the 12th World Conference on Earthquake Engineering, 2000.
6. Kobayashi, H. and Midorikawa, S., "A Semi-Empirical Method for Estimating Response Spectra of Near-Field Ground Motions with regard to Fault Rupture," Proc. of the 7th European Conference on Earthquake Engineering, pp.161-168, 1982.
7. Nishimura, I., Noda, S., Takahashi, K., Takemura, M., Ohno, S., Tohdo, M. and Watanabe, T., "Response Spectra for Design Purpose of Stiff Structures on Rock Sites," Transactions, SMiRT 16, Paper# 1133, 2001.
8. Kinoshita, S., "Kyoshin Net (K-NET),"Seism. Res. Left., 69, pp.309-332, 1998.
9. Takemura, M., "Magnitude - Seismic Moment Relations for the Shallow Earthquakes in and around Japan, "Zisin, 2nd Series, 43, pp.257-265, 1990 (in Japanese with English Abstract).
10. Kato, K., Takemura, M., Ikeura, T. and Yashiro, K., "Excitation Strength of High-frequency Seismic Motion due to Intermediate Depth Earthquakes," Proc. of the 10th Japan Earthquake Engineering Symposium, pp.673-678, 1998 (in Japanese with English Abstract).
11. Ohno, S., Takemura, M. and Kobayashi, Y., "Effects of Rupture Directivity on Near-Source Strong Motions," Proc. of the 2nd International Symposium on the Effects of Surface Geology on Seismic Motion, pp. 1163-1170, 1998.

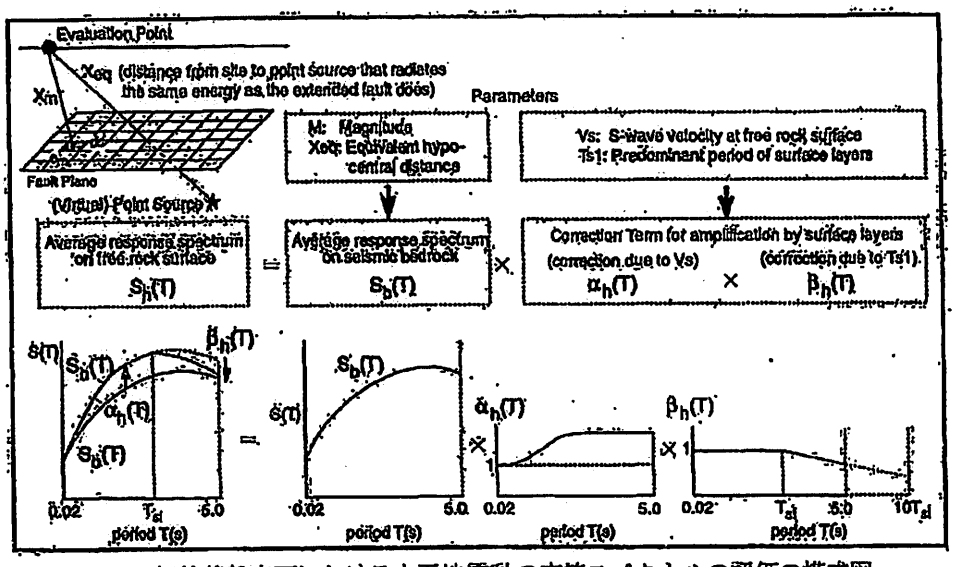

図１　解放基盤表面における水平地震動の応答スペクトルの評価の模式図

表１　地震基盤における水平地震動のコントロールポイント

Field	M	Xeq (km)	Coordinates of Control Points pSv (cm/s)							
			A	B	C	D	E	F	G	H
			TA(s)	TB(s)	TC(s)	TD(s)	TE(s)	TF(s)	TG(s)	TH(s)
			0.02	0.09	0.13	0.3	0.6	1	2	5
Very Near	8.5	40	1.62	18.44	27.32	47.87	68.65	64.66	53.52	40.06
	8	25	1.69	20.05	28.96	48.22	67.80	65.25	52.51	38.35
	7	12	1.40	17.20	24.84	33.86	43.42	36.42	25.15	17.85
	6	5	1.04	12.82	18.51	21.84	23.17	17.41	9.64	3.88
Near	8.5	80	0.78	7.66	11.43	22.92	34.79	32.58	27.60	21.96
	8	50	0.67	7.45	11.17	20.05	28.65	27.06	22.70	17.19
	7	20	0.78	9.44	13.84	19.10	24.83	20.69	14.48	10.37
	6	8	0.77	9.45	13.65	16.23	17.18	12.73	7.16	2.89
Inter mediate	8.5	160	0.26	2.22	3.67	9.45	15.17	14.83	13.64	12.26
	8	100	0.32	3.08	4.86	10.27	16.04	14.96	12.73	10.37
	7	50	0.23	2.65	4.01	6.02	7.64	6.66	4.87	3.64
	6	25	0.21	2.49	3.80	4.54	4.84	3.98	2.07	0.86
Far	8.5	200	0.18	1.44	2.43	6.87	11.17	11.17	10.87	10.04
	8	200	0.10	0.80	1.35	3.82	6.21	6.21	5.93	5.58
	7	125	0.046	0.43	0.70	1.94	1.81	1.59	1.26	1.05
	6	78	0.041	0.45	0.65	0.95	1.03	0.80	0.49	0.22

The value of pSv is pseudo-velocity response spectrum with a damping factor of 5%.

表２　係数 $\delta_h(T)$，$\delta_v(T)$，$\alpha_{bv}(T)$

	A	B	C	D	E	F	G	H
	TA(s)	TB(s)	TC(s)	TD(s)	TE(s)	TF(s)	TG(s)	TH(s)
	0.02	0.09	0.13	0.3	0.6	1	2	5
$\delta_h(T)$	0	0.03	0.05	0.35	0.48	0.61	0.80	0.83
$\delta_v(T)$	0.12	0.26	0.42	0.67	0.90	1.03	1.10	1.09
$\alpha_{bv}(T)$	0.58	0.55	0.52	0.59	0.56	0.60	0.70	0.75

The coefficients are common for all combinations of M and Xeq

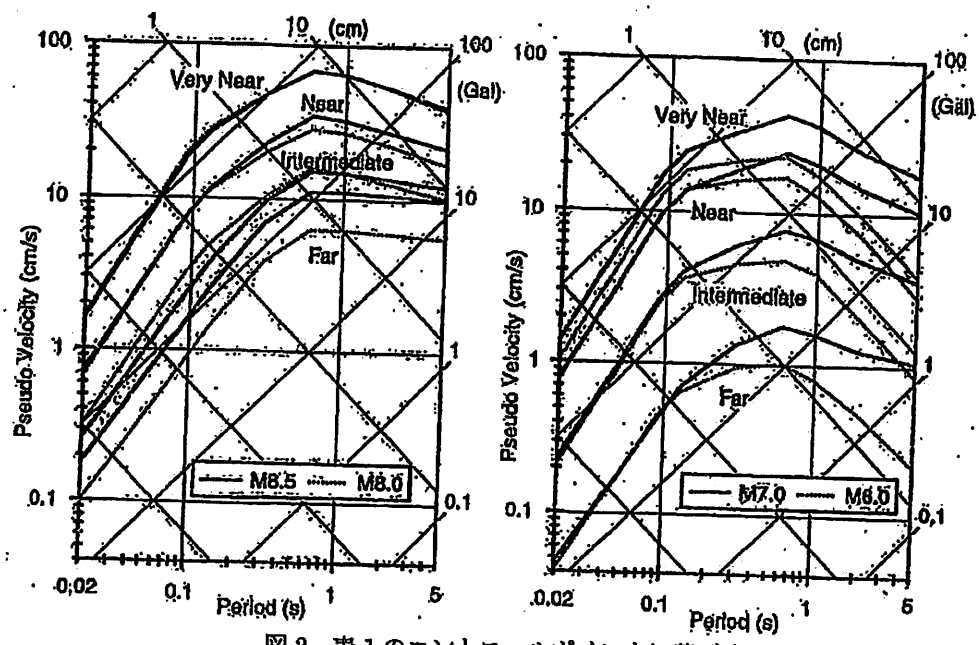

図２　表１のコントロールポイントに基づく
地震基盤における水平地震動の応答スペクトル

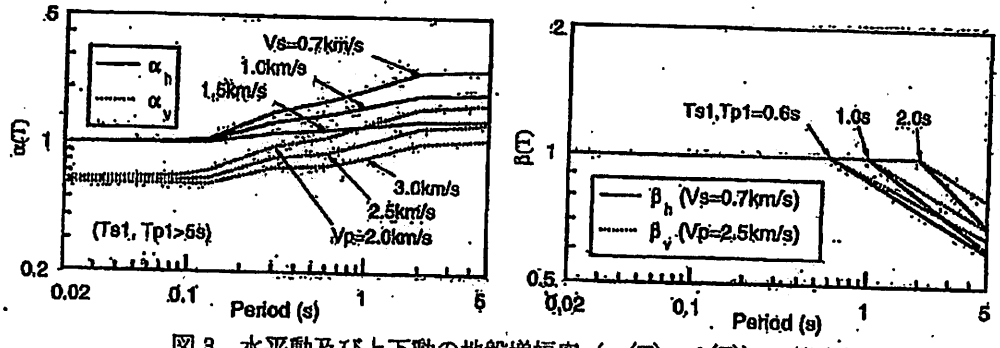

図３　水平動及び上下動の地盤増幅率（α(T)，β(T)）の算定例

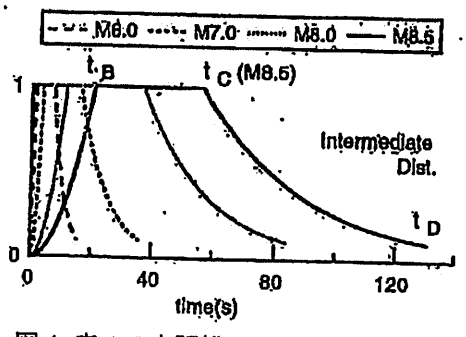

図４　表１の中距離のコントロールポイントに基づく包絡線

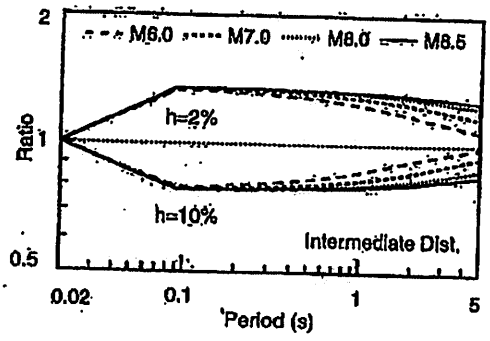

図５　表１の中距離のコントロールポイントに基づく異なる減衰定数の応答スペクトルの補正係数

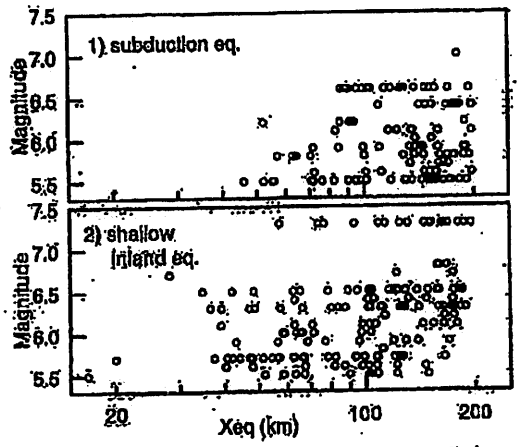

図 6　図 8 の分析に用いた M - X_{eq} 分布

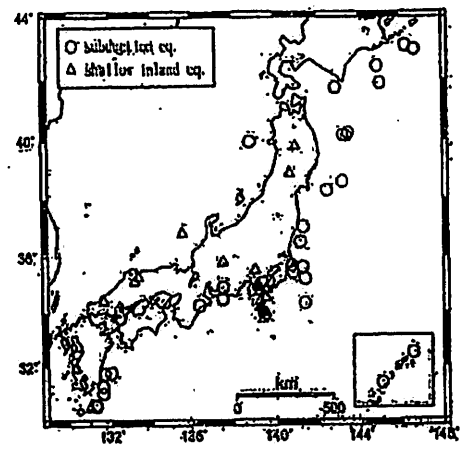

図 7　図 8 の分析に用いた地震の震央分布

表 3　分析に用いたデータ範囲

	Data for regression analysis in Ref. 4,5	Data for applicability check in Ref.7	Data used in this paper	
			subduction eq.	shallow inland eq.
Magnitude	5.5 - 7.0	5.4 - 8.1	5.5 - 7.0	5.5 - 7.3
Xeq (km)	28 - 202	14 - 218	46 - 199	17 - 195
Vs (m/s)	≥500	≥550	≥700	≥500
Number of Records	107	37	124	170

All data satisfy 1).Focal depth ≤ 60km, 2).Observation sites belong to stratum of tertiary or older.

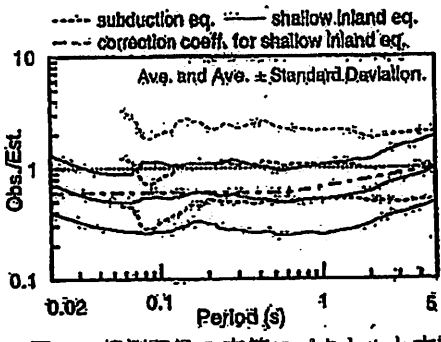

図 8　観測記録の応答スペクトルと本評価法による応答スペクトルの比

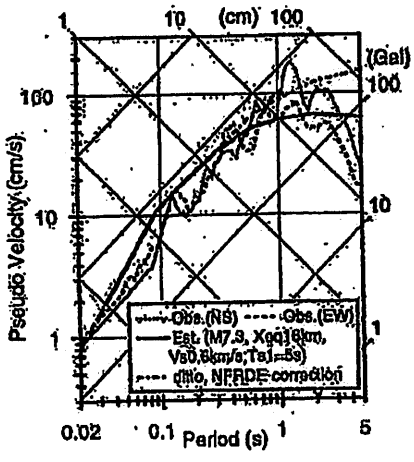

(1) 1995 Hyogo-ken Nanbu (Kobe) Eq., Kobe Univ. station, Japan

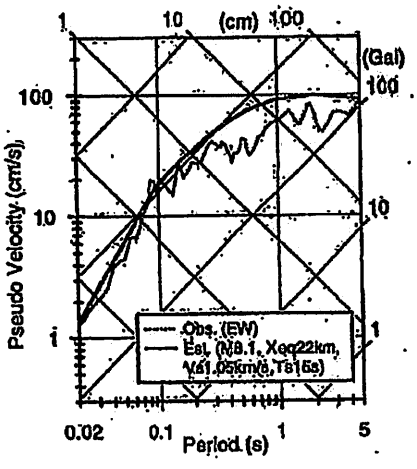

(2) 1999 Kocaeli Eq., Sakarya station, Turkey

図 9　震源近傍の観測記録に対する本評価手法の適用例